Published in final edited form as:

Pharmacol Res. 2018 March ; 129: 515–525. doi:10.1016/j.phrs.2017.11.036.

Functional histamine H_3 and adenosine A_{2A} receptor heteromers in recombinant cells and rat striatum

Ricardo Márquez-Gómez[a], **Meridith T. Robins**[c], **Citlaly Gutiérrez-Rodelo**[b], **Juan-Manuel Arias**[d], **Jesús-Alberto Olivares-Reyes**[b], **Richard M. van Rijn**[c], and **José-Antonio Arias-Montaño**[a]

[a]Departamentos de Fisiología, Biofísicay Neurocienciasy, Av. IPN 2508, Zacatenco, 73063 Ciudad de México, México

[b]Departamentos de Bioquímica, Cinvestav-IPN, Av. IPN 2508, Zacatenco, 73063 Ciudad de México, México

[c]Department of Medicinal Chemistry and Molecular Pharmacology, Purdue University, West Lafayette, IN, USA

[d]Programa de Neurociencias-UIICSE, Facultad de Estudios Superiores Iztacala, UNAM, Av. de los Barrios 1, Los Reyes Iztacala, 54090 Estado de México, México

Abstract

In the striatum, histamine H_3 receptors (H_3Rs) are co-expressed with adenosine A_{2A} receptors (A_{2A}Rs) in the cortico-striatal glutamatergic afferents and the GABAergic medium-sized spiny neurons that originate from the indirect pathway of the basal ganglia. This location allows H_3Rs and A_{2A}Rs to regulate the striatal GABAergic and glutamatergic transmission. However, whether these receptors can physically interact has not yet been assessed. To test this hypothesis, a heteromer-selective *in vitro* assay was used to detect functional complementation between a chimeric $A_{2A}R_{302}$-$G\alpha_{qi4}$ and wild-type H_3Rs in transfected HEK-293 cells. H_3R activation with the agonist RAMH resulted in Ca^{2+} mobilization (pEC_{50} 7.31 ± 0.23; maximal stimulation, Emax 449 ± 25% of basal) indicative of receptor heterodimerization. Functional H_3R-A_{2A}R heteromers were confirmed by co-immunoprecipitation and observations of differential cAMP signaling when both receptors were co-expressed in the same cell. In membranes from rat striatal synaptosomes, H_3R activation decreased A_{2A}R affinity for the agonist CGS-21680 (pKi values 8.10 ± 0.04 and 7.70 ± 0.04). Moreover, H_3Rs and A_{2A}Rs co-immunoprecipitated in protein extracts from striatal synaptosomes. These results support the existence of a H_3R-A_{2A}R heteromer with possible physiological implications for the modulation of the intra-striatal transmission.

Corresponding author: Ricardo Márquez-Gómez M. Sc., Departamento de Fisiología, Biofísica y Neurociencias, Cinvestav-IPN, Av. IPN 2508, Zacatenco, 07360, Ciudad de México, México, Tel. (+5255) 5747 5706, ricardo.marquez3@gmail.com.

Author contributions

R. M.-G., R. v. R. and J.-A. A.-M. designed the study; R. M.-G., C. G.-R., J.-M. A. and M. T. R. performed the experiments; R. M.-G., J.-A. O.-R., R. v. R. and J.-A. A.-M. performed data analysis. R. M.-G., R. v. R. and J.-A. A.-M. wrote the manuscript. All authors revised and approved the manuscript.

Conflicts of interest

The authors disclose no conflict of interest.

Keywords

Adenosine A_{2A} receptor; histamine H_3 receptor; striatum; GPCR heterodimers; basal ganglia

1. Introduction

The actions of histamine in the periphery on airway constriction, inflammation and gastric acid secretion are well known, whereas its function in the Central Nervous System (CNS) is not yet fully understood. In mammals, histamine actions are mediated by four (H_1R-H_4R) G protein-coupled receptors (GPCRs), of which the H_3 receptor (H_3R) displays the highest expression in the brain. In the CNS, histamine is released from the terminals and dendrites of neurons located in the hypothalamic tuberomammilary nucleus, from where they innervate most of the CNS, including nuclei belonging to the basal ganglia, a subcortical group of structures intimately related to the control of motor behavior (Panula and Nuutinen, 2013; Panula *et al.*, 2015).

The striatum is the main input nucleus of the basal ganglia and integrates motor and sensory information. The primary striatal afferents are glutamatergic axons originating from neurons located in the cerebral cortex and thalamus, and dopaminergic axons of sustantia nigra pars compacta neurons (Bolam *et al.*, 2000). In turn, the axons of the GABAergic medium-sized spiny neurons (MSNs), which account for more than 90% of the striatal neuronal population (Kemp and Powell, 1971), project to the globus pallidus and sustantia nigra pars reticulata (Bolam *et al.*, 2000).

H_3Rs are abundantly expressed in the striatum either as pre-synaptic auto- and hetero-receptors or as post-synaptic receptors, with the latter located on the bodies of the MSNs and GABAergic or cholinergic interneurons (Pillot *et al.*, 2002; González-Sepúlveda *et al.*, 2013; Bolam and Ellender, 2016). The understanding of the physiological role of striatal H_3Rs is complicated by their ubiquitous expression and capability to engage in protein-protein interactions with other GPCRs (Nieto-Alamilla *et al.*, 2016). Of particular interest in the striatum are dopamine and adenosine receptors, which are also highly expressed. Based on the selective expression of dopamine and adenosine receptor subtypes, MSNs can be segregated into two neuronal populations. Neurons that originate the basal ganglia direct pathway (dMSNs) are identified by the expression of D_1-like receptors (D_1Rs) whereas the indirect pathway population (iMSNs) is formed by neurons expressing adenosine A_{2A} receptors (A_{2A}Rs) and D_2-like receptors (D_2Rs) (Schiffman *et al.*, 1991; Ferre *et al.*, 1997; Tapper *et al.*, 2004). In the striatum, H_3Rs have been shown to form heterodimeric protein-protein complexes with dopamine D_2 and D_1 receptors (Ellenbroek, 2013), and heterotrimers with $\sigma1$/D_1 receptors and NMDA/D_1 receptors (Moreno *et al.*, 2014; Rodríguez-Ruíz *et al.*, 2016). In turn, A_{2A}Rs can form dimers with D_2, cannabinoid CB_1 and adenosine A_1 receptors (Ciruela *et al.*, 2006; Carriba *et al.*, 2007; Hillon *et al.*, 2002) and oligomers with D_2 and mGlu5 glutamate receptors (Cabello *et al.*, 2009).

Both H_3 and A_{2A} receptors modulate intra-striatal synaptic transmission. The activation of $G\alpha_{i/o}$-coupled H_3Rs results in inhibition of GABA, dopamine, acetylcholine and glutamate release (Doreulee *et al.*, 2001; Schlicker *et al.*, 1993; Prast *et al.*, 1999; Arias-Montaño *et al.*,

2001), whereas the activation of $G\alpha_s$-coupled A_{2A}Rs also inhibits GABA release but facilitates glutamatergic cortico-striatal transmission (Kirk and Richardson, 1994; Popoli *et al.*, 1995).

Either individually or through their heteromeric interactions with other GPCRs, A_{2A}Rs and H_3Rs have been proposed as targets for the treatment of basal ganglia-related disorders such as Parkinson's disease and addiction (Ferré *et al.*, 2004; Schwarzschild *et al.*, 2006; Passani and Blandina, 2011; Ellenbroek, 2013). In this work, we hypothesized that striatal H_3Rs and A_{2A}Rs can not only form heteromers with dopamine receptors, but also with each other, and that this interaction forms a unique pharmacological target that could be of potential therapeutic interest. Here we show that H_3Rs co-immunoprecipitate with A_{2A}Rs in HEK293 cells, suggestive of oligomerization. Further, we studied the physical properties of the A_{2A}R-H_3R interaction by a functional complementation assay. We next showed that the A_{2A}R-H_3R heteromerization has unique functional pharmacology in terms of cAMP modulation in HEK-293 cells co-expressing the receptors. Using protein extracts from striatal synaptosomes, we confirmed the presence of A_{2A}R-H_3R heteromers *in vivo* by co-immunoprecipitation. Finally, we found that in the same preparation H_3R activation resulted in decreased binding affinity of A_{2A}R for the agonist CGS-21680.

A preliminary account of this work was presented in the abstract form to the European Histamine Research Society (Márquez-Gómez *et al.*, 2016) and submitted to an electronic pre-print server (Márquez-Gómez *et al.*, 2017).

2. Methods

2.1 Materials

The following drugs and reagents were purchased from Sigma Aldrich (St. Louis, MO, USA): (R)(−)-α-methylhistamine dihydrochloride, histamine dihydrochloride, adenosine deaminase (from bovine spleen), Percoll, quinpirole dihydrochloride. Dimaprit was from Axon MedChem (Reston, VA, USA). CGS-21680 was from Cayman Chemical (Ann Arbor, MI, USA). N-α-[methyl-^{3}H]-histamine (78.3 Ci·mmol^{-1}) and CGS-21680-[carboxyethyl-^{3}H(N)]-(35.2 Ci·mmol^{-1}) were from Perkin Elmer (Boston, MA, USA).

2.2 Molecular cloning

Truncated A_{2A} or H_3 receptors were generated by PCR using the primers indicated in Supplementary Table 1. After amplification and restriction with HindIII and BamHI enzymes, the truncated A_{2A} and H_3 receptors were ligated to a pcDNA3.1 plasmid that contained the chimeric $G\alpha_{qs4}$ and $G\alpha_{qi4}$ proteins. Both A_{2A}Rs and H_3Rs (cDNA Resource Center, Bloomsberg, PA, USA) were labeled with a triple hemagglutinin tag (3xHA). To generate the 3xHA tagged receptors, A_{2A}R and the H_3R were amplified from nucleotide 377 and 458, respectively, towards their amino terminus. The 3xHA tag was amplified from a plasmid that codified for the tagged histamine H_4R (3xHA-H_4R in pcDNA3.1, cDNA Resource Center). The amplified DNA fragments (3xHA-A_{2A}R377/H_3R458) where then re-introduced into the pcDNA3.1-H_3R or pcDNA3.1-A_{2A}R backbone to obtain the tagged, full length receptors. The insertion and orientation of the amplified fragment was verified by

automated sequencing performed at FESI-UNAM (Los Reyes Iztacala, Estado de México, México).

2.3 Cell culture and transfection

HEK-293T cells (American Type Culture Collection, Manassas, VA, USA) were grown in Dulbecco's Modified Eagle's Medium (DMEM) supplemented with 10% fetal bovine serum (FBS), penicillin (50 UI/ml) and streptomycin (0.1 mg/ml) under a humidified atmosphere (5% CO_2 in air) at 37 °C.

For transfections, cells were seeded in 6-well plates (6×10^5 cells/well; up to passage 15) and incubated for 24 h at 37 °C in a 5% CO_2/air mixture. The next day, 10 μl X-tremeGENE (Roche, Basilea, Switzerland) were mixed with 500 μl Optimem (Life Technologies, San Diego, CA, USA) and the mixture was incubated for 5 min at room temperature before the addition of cDNA in a 1:5 ratio with X-tremeGENE. For cAMP assays a mixture of DNA:Glosensor cAMP plasmid (1:2 ratio) was added to the Optimem/X-tremeGENE solution. When plasmids containing the $A_{2A}R$ or H_3R were transfected alone, the amount of DNA was preserved by adding empty pcDNA3.1 vector. The transfection mixture was incubated for 20 min at room temperature and then added to the cells, which were incubated for 24 h at 37 °C under a humidified atmosphere (5% CO_2/air).

For co-immunoprecipitation assays, HEK-293T cells, grown in 100-millimeter Petri dishes and at 80% confluence, were transfected using the Lipofectamine 2000 method. Briefly, a mixture of DNA/Lipofectamine 2000 (1:2 ratio) was incubated for 20 min at room temperature before being added to the cells. After incubation for 5 h at 37 °C under a humidified atmosphere (5% CO_2/air), the medium was replaced by high-glucose DMEM supplemented with 10% FBS and 1% antibiotic/antimycotic. Incubation continued for a further 24 h under the same condition.

2.4 cAMP accumulation assay

cAMP assays were performed as described in detail elsewhere (Chiang *et al.*, 2016). Briefly, HEK-293T cells transfected with 3xHA-$A_{2A}R$, 3xHA-H_3R or a mixture of both plasmids (1 μg each) together with Glosensor cAMP plasmid (Promega, Madison, WI, USA) were seeded in a white 384-well low-volume plate (25,000 cells/well in 7.5 μl medium) and incubated with Glo-equilibrium medium (7.5 μl, Promega). Drugs under test were added in a 5 μl volume (4x in HBSS solution) and endogenous cAMP luminescence was measured in real-time in a Flexstation 3 apparatus (Molecular Devices, Sunnyvale, CA, USA).

2.5 Calcium mobilization assay

HEK-293T cells transfected with 1 μg of DNA were seeded (2.5×10^4 cells/well) in a 384-well clear bottom black plate (25 μl-volume) and incubated for 24 h at 37 °C in a humidified 5% CO_2/air atmosphere, covered with Areaseal film (Sigma, St. Louis, MO, USA). Cells were then loaded with 25 μl of the FLIPR Ca^{2+} dye (Molecular Devices, Sunnyvale, CA, USA) and incubated for 1 h at 37 °C. Agonists were added in a 20 μl volume and calcium mobilization was measured in real-time for 2 min in a Flexstation 3 apparatus (Molecular Devices, Sunnyvale, CA, USA) and analyzed as described in detail in van Rijn *et al.* (2013).

2.6 Synaptosome preparation

All procedures were approved and controlled by the Cinvestav Animal Care Committee and were in accord with the rules issued by the National Institutes of Health (NIH Publications No. 8023) and the Mexican Council for Animal Care. Wistar rats (males, 250–300 g, provided by Unidad de Producción y Experimentación para Animales de Laboratorio; Cinvestav, Mexico City) were decapitated, the brain was quickly removed from the skull and the forebrain was separated and deposited on a metal plate placed on ice. The striata from 3–5 animals were dissected using forceps and the whole tissue was placed in 5 ml 0.32 M sucrose solution containing 10 mM Hepes, 1 mg/ml bovine serum albumin and 1 mM EDTA (pH 7.4 with NaOH). The tissue was homogenized using 10 strokes of a hand-held homogenizer (400 rpm), the homogenate was centrifuged (1000x*g*, 10 min, 4 °C) and the supernatant was pelleted at 14,000x*g* (12 min, 4 °C). The pellet was re-suspended in 5 ml of a Percoll solution (45 %, v:v) in Krebs-Henseleit-Ringer buffer (in mM: NaCl 140, Hepes 10, D-glucose 5, KCl 4.7, EDTA 1, pH 7.3 with NaOH). After centrifugation (2 min, 14,000x*g*, 4 °C), the upper phase was collected and brought up to 20 ml with Krebs-Ringer-Hepes (KRH) solution (in mM: NaCl 113, $NaHCO_3$ 25, Hepes 20, D-glucose 15, KCl 4.7, $CaCl_2$ 1.8, $MgCl_2$ 1.2, KH_2PO_4 1.2, pH 7.4 with NaOH). The suspension was centrifuged (20,000x*g*, 20 min, 4 °C) and the pellet (synaptosomes) was re-suspended in KRH solution unless otherwise indicated.

2.7 Electron microscopy

Striatal synaptosomes were isolated by the Percoll method as above. Sample preparation and electron microscopy were performed as described in detail elsewhere (Morales-Figueroa *et al.*, 2015).

2.8 Radioligand binding assays with striatal membranes

Striatal synaptosomes were re-suspended in lysis solution (Tris-HCl 10 mM, EGTA 1 mM, pH 7.4) and incubated for 20 min at 4 °C before centrifugation (20 min, 20,000xg, 4 °C). The pellet (synaptosomal membranes) was re-suspended in 1 ml KRH solution containing adenosine deaminase (2 U/ml). After incubation for 30 min at 37 °C, the suspension was brought to 20 ml with KRH solution and centrifuged (20 min, 20,000x*g*, 4 °C). The membranes were re-suspended in incubation solution (Tris-HCl 50 mM, $MgCl_2$ 5 mM, pH 7.4) and 130 μl aliquots (40 μg protein) were incubated with 10 μl of increasing concentrations of CGS-21680 or RAMH (20x) and 50 μl of [^{3}H]-NMHA (8 nM) or [^{3}H]-CGS-21680 (48 nM). After 1 h at 30 °C ([^{3}H]-NMHA) or 2 h at 25°C ([^{3}H]-CGS-21680), incubations were stopped by rapid filtration through Whatman GF/B filters pre-soaked (2 h) in 0.3 % polyethylenimine (PEI). Filters were washed 3 times with 1 ml ice-cold buffer solution (50 mM Tris-HCl, pH 7.4), soaked in 4 ml scintillation solution and the tritium content was determined by scintillation counting.

2.9 Co-immunoprecipitation assays

Striatal synaptosomes were obtained as described above and then re-suspended in 1 ml of lysis solution (Tris-HCl 50 mM, NaCl 150 mM, Triton X-100 1%, SDS 0.05%, protease inhibitor 1 μl/ml). HEK-293T cells were dislodged in RIPA solution. For both synaptosomal

and cell samples, protein was extracted by sonication (3 cycles, 30 sec, 8 kHz). The sample was centrifuged (20 min, 6,000x*g*) and the protein extract (supernatant) was collected. Nonspecific binding was removed by incubation (1 h, 4 °C) with 10 μl of AG beads (Santa Cruz Biotechnology; Dallas, TX, USA) under rotatory rocking. The beads were pelleted (2 min, 6000x*g*) and the supernatant was used for the assay. Protein quantification was performed by the BCA method.

The protein extracts (500 μg protein from striatal synaptosomes and 200 μg from HEK-293T) were incubated with 2 μg of the primary antibodies (anti-A_{2A}R Abcam, cat. ab3461, lot. GR238882–9; anti-H_3R, Abcam, cat. ab84468, lot. GR27494–1, in a 1:100 dilution) together with AG beads (Santa Cruz Biotechnology sc-2003, 1:5 antibody to beads ratio) for 16 h at 4°C with constant rotational rocking. Antibodies against the CD-81 protein (Santa Cruz Biotechnology, cat. sc-70803, lot. B0609) or D_2R (Santa Cruz Biotechnology, cat. sc-5303, lot. A03013) were used as negative controls for the striatal synaptosomes or HEK-293T cells, respectively. The bead-antibody complex was pelleted (2 min, 6000x*g*) and a 30 μl aliquot of the supernatant was used as a load control. In both protein extracts, 30 μl of the total protein was used as input. The complex was dissociated for 60 min at 48°C in loading buffer (10% β-mercaptoethanol and 50% Laemmli buffer in H_2O) and separated by electrophoresis in a 10% SDS-polyacrylamide gel (20 min at 80 V and then 65 min at 120 V). Semi-dry transfer was performed at 15 V for 95 min. Membranes were blocked with 5% nonfat dry milk diluted in TBS-Twin 0.05% solution (overnight, 4°C). After extensive washing, 5 ml of TBS-Twin 0.05% solution containing 5% BSA and the blotting antibody (anti-A_{2A}R, anti-HA, Cell Signaling, cat. C29F4, lot. 3724S or anti-H_3R, in a 1:1000 dilution) were added to the membrane and incubated overnight at 4 °C. Membranes were incubated with the secondary antibody (Invitrogen, HRP-conjugated anti-rabbit IgG, cat. 65–6120, 1:5000, non-fat dry milk 5% in TBS-Twin 0.05%) at room temperature for 2 h. For the loading controls membranes were incubated for 1 h with antibodies directed to β-tubulin (Invitrogen, cat. 322600, lot. 1235662) or α-actin (Sigma, cat. A5228, lot. 128K4843) in a 1:5000 dilution in TBST 0.05%. After washing, membranes were incubated for 1 h with the secondary antibody (α-mouse, Santa Cruz, cat. sc-2005) diluted in TBST 0.05%. Blot images were obtained by chemiluminescence in an X-ray film (Kodak).

2.10 Statistical analysis

Data show the mean ± standard error of the mean (SEM). Statistical analysis was performed with student *t*-test with Prisma GraphPad software, version 5.0 (San Diego, CA, USA).

3. Results

3.1 Co-immunoprecipitation of A_{2A}Rs and H_3Rs expressed in HEK-293 cells

We first studied by co-immunoprecipitation whether H_3Rs and A_{2A}Rs interact physically upon co-transfection in HEK-293T cells. 3xHA-H_3Rs were detected after immunoprecipitation of wild type (WT) A_{2A}Rs (Figure 1A). HEK-293T cells lack expression of the D_2 receptor, and an antibody targeting this receptor was therefore used as a negative control, yielding no signal. This result supports dimerization between H_3Rs and A_{2A}Rs.

3.2 Functional complementation of A_{2A}Rs and H_3Rs expressed in HEK-293 cells

To further study the potential interaction between A_{2A}Rs and H_3Rs in a recombinant cell system, we employed a functional complementation assay, previously used to study physical interactions between GPCRs (Han *et al.*, 2009; van Rijn *et al.*, 2013). This assay relies on the fusion of chimeric $G\alpha_{qs4}$ or $G\alpha_{qi4}$ proteins to the truncated C-terminal tail of a GPCR to generate a nonfunctional receptor, rescuable through homo- or hetero-dimerization with a WT, untruncated receptor. It was previously reported that fusion of a chimeric G protein to a GPCR truncated near helix 8 produces a receptor that is unable to signal by itself but can be rescued when transfected with a full-length receptor (van Rijn *et al.*, 2013). Therefore, we first generated an A_{2A}R truncated to 302 residues ($A_{2A}R_{302}$) and H_3Rs of 427, 421 and 411 residues (H_3R_{427}, H_3R_{421} and H_3R_{411}), and the truncated receptors were then fused to the chimeric G proteins (Figure 2A).

Activation of the H_3R in transfected CHO-K1 cells and rat striatal neurons in primary culture induces Ca^{2+} mobilization (Cogé *et al.*, 2001; Rivera-Ramirez *et al.*, 2016), and in the striatum A_{2A}R activation favors Ca^{2+} entry by modulating voltage-activated Ca^{2+} channels (Kirk and Richardson, 1995; Gubitz *et al.*, 1996), which are endogenously expressed by HEK-293 cells (Berjukow *et al.*, 1996; Thomas and Smart, 2005). In HEK-293 cells, the H_3R selective agonist RAMH did not induce any discernible Ca^{2+} response but did so when the H_3R was co-transfected with $G\alpha_{qi4}$ proteins (Figure 2B). The A_{2A}R did not induce Ca^{2+} signaling when activated by the selective agonist CGS-21680, but also no response was observed when co-transfected with $G\alpha_{qs4}$ proteins, suggesting that A_{2A}Rs do not activate this chimeric protein (Figure 2C). It has been reported that not all GPCRs are amenable to signal through chimeric G-proteins (Conklin *et al.*, 1996). A different $G\alpha_s$-coupled receptor, the histamine H_2 receptor, was capable to induce Ca^{2+} release when co-transfected with $G\alpha_{qs4}$ proteins and stimulated with the selective agonist dimaprit (Supplementary Figure 1A), discarding $G\alpha_{qs4}$ malfunction. Consistent with the finding that A_{2A}Rs did not signal efficiently via chimeric G-proteins, functional complementation by homodimerization of $A_{2A}R_{302}$-$G\alpha_{qs4}$ or $A_{2A}R_{302}$-$G\alpha_{qi4}$ with the full-length A_{2A}R was not observed (Figure 2D).

The C-tail of the H_3R was truncated such that the H_3R-$G\alpha_{qi4}$ fusion protein would display limited Ca^{2+} mobilization when expressed alone, but a pronounced Ca^{2+} signaling when co-expressed with WT-H_3Rs. The H_3R_{421}-$G\alpha_{qi4}$ and the H_3R_{411}-$G\alpha_{qi4}$ constructs did not induce Ca^{2+} mobilization, and could not be rescued via homo-dimerization with WT-H_3Rs (Supplementary Figure 1B). However, Ca^{2+} mobilization induced by H_3R_{427}-$G\alpha_{qi4}$ upon activation and co-transfection with WT-H_3Rs produced a similar increase in calcium release (Figure 2E). While not optimal, this behavior allowed for the study of the interaction between the H_3R_{427}-$G\alpha_{qi4}$ and the A_{2A}R as described below.

Co-transfection of the 'inert' $A_{2A}R_{302}$-$G\alpha_{qi4}$ and H_3Rs induced Ca^{2+} mobilization after activation of the latter receptors with RAMH, suggestive of close physical proximity between the H_3R and both the A_{2A}R and the fused $G\alpha_{qi4}$-protein. H_3R activation failed to induce functional complementation in cells co-transfected with $A_{2A}R_{302}$-$G\alpha_{qs4}$ (Figure 3A). Given that H_3Rs are $G\alpha_{i/o}$-coupled, and the inability of the A_{2A}R to signal through chimeric $G\alpha_{qi4}$- or $G\alpha_{qs4}$-proteins, it was not surprising that A_{2A}R activation with the selective

agonist CGS-21680 did not produce any response through H_3R_{427}-$G\alpha_{qs4}$ or H_3R_{427}-$G\alpha_{qi4}$ (Figure 3B). Interestingly, the co-expression of WT-A_{2A}Rs prevented RAMH-induced Ca^{2+} mobilization mediated by the H_3R_{427}-$G\alpha_{qi4}$ (compare Figure 2E and Figure 3C). We briefly explored this pharmacological response further by analyzing Ca^{2+} mobilization in HEK-293T cells co-expressing the H_3R_{427}-$G\alpha_{qi4}$ and the $A_{2A}R$ or the $A_{2A}R_{302}$-$G\alpha_{qi4}$ and the H_3R and activating both receptors, but did not observe any additive or antagonistic effect (Supplementary Figure 1C and 1D).

A_{2A}Rs have been shown to form heteromers with D_2Rs (Ferré *et al.*, 2003) and robust functional complementation was accordingly observed when $A_{2A}R$-$G\alpha_{qi4}$ was co-expressed with WT-D_2Rs (Figure 3D), supporting that our results are due to heterodimerization and not to stochastic interactions.

3.3 The putative $A_{2A}R$-H_3R heteromer displays ligand bias

To test for the selective nature of the $A_{2A}R$-H_3R interaction in the functional complementation assay, we investigated if $A_{2A}R$-$G\alpha_{qi4}$ would also allow the structurally and physiologically similar histamine H_4 receptor (H_4R) to induce Ca^{2+} signaling. Co-activation with histamine of H_3Rs and H_4Rs elicited Ca^{2+} mobilization only when co-transfected with $G\alpha_{qi4}$ (Supplementary Figure 2A and 2B, respectively). Neither histamine nor RAMH induced Ca^{2+} mobilization when the H_4R was co-expressed with $A_{2A}R_{302}$-$G\alpha_{qi4}$, supporting the specificity of the $A_{2A}R$-H_3R interaction (Figure 3E). Unexpectedly, whereas RAMH induced Ca^{2+} mobilization when the H_3R was co-expressed with $A_{2A}R_{302}$-$G\alpha_{qi4}$, histamine did not (compare Figure 3A with Figure 3F). This result suggests that the $A_{2A}R$-H_3R heteromer displays agonist bias.

3.4 $A_{2A}R$-mediated signaling is increased by H_3R co-activation

To study the pharmacology of the putative $A_{2A}R$-H_3R heteromer we next tested cAMP signaling using WT receptors in HEK-293T cells. In cells transfected with the $A_{2A}R$, incubation with CGS-21680 resulted in a concentration-dependent increase in cAMP levels in accordance with the receptor's coupling to the $G\alpha_s$ signaling pathway (Figure 3A). CGS-21680 induced a similar cAMP response in HEK293T-$A_{2A}R$ cells co-expressing H_3Rs (Figure 4A). Co-activation of the receptors resulted in a decrease in baseline, in agreement with the $G\alpha_{i/o}$ coupling of the H_3R, but led to an augmentation of $A_{2A}R$-mediated cAMP formation as noticed by a 2.5-fold change of baseline (versus 1.5-fold in control). This result suggests that the $A_{2A}R$ signaling becomes more efficacious when heterodimerization with the H_3R occurs (Figure 4A, Supplementary Figure 2C, and Table 2). The increase in the $A_{2A}R$ signaling was not observed in the absence of RAMH (1.5-fold of baseline) suggesting an agonist-dependency of the response (Figure 4A and Supplementary Figure 2C).

In HEK293T-H_3R cells, RAMH inhibited forskolin-stimulated cAMP formation congruent with the $G\alpha_{i/o}$ coupling of the H_3R receptor. However, when the $A_{2A}R$ was co-transfected, RAMH-mediated H_3R signaling shifted to facilitate cAMP formation instead. Activation of the $A_{2A}R$ caused an expected increase in the baseline but did not significantly modify the effect on cAMP formation. This result suggests that in the heterodimer, $A_{2A}R$ signaling prevails over the H_3R signaling (Figure 4B and Supplementary Figure 2D; Table 2).

3.5 H_3R activation decreases $A_{2A}R$ binding affinity in synaptosomal membranes

The identification of $A_{2A}R$-H_3R heteromers was performed in recombinant cell systems over-expressing the receptors. As previously mentioned $A_{2A}Rs$ and H_3Rs are co-expressed in iMSNs and cortico-striatal projections. We therefore used rat striatal synaptosomes to seek for pharmacological traces that supported the existence of native $A_{2A}R$-H_3R dimers.

Electron microscopy confirmed in the purified synaptosomal preparation the vast presence and conserved structure of isolated nerve terminals, characterized by a delimited membrane and the presence of mitochondria and synaptic vesicles (Supplementary Figure 3A and B). In protein extracts from striatal synaptosomes, immunoprecipitation of the $A_{2A}R$ resulted in a band of ~45 kDa, corresponding to the expected migration of the H_3R. No signal was detected when an irrelevant antibody (α-CD81) was tested. As a positive control the H_3R was immunoprecipitated and detected as a band of ~45 kDa (Figure 5A). When the reverse approach was employed and the H_3R was immunoprecipitated from the striatal protein extracts, a band of ~45 kDa corresponding to the expected migration of the $A_{2A}R$ was observed. This band was also observed when the $A_{2A}R$ was immunoprecipitated as a positive control but not detected in the negative control (Figure 5B). This result supports that the interaction $A_{2A}R$-H_3R is constitutively present in the striatal nerve terminals.

In binding studies with synaptosomal membranes the $A_{2A}R$ agonist CGS-21680 (10 and 100 nM) did not affect the affinity of the H_3R for its agonist RAMH (Figure 6A), whereas RAMH (100 nM) decreased by two-fold the affinity of the $A_{2A}R$ for CGS-21680 (Figure 6B, 6C and Table 3), with no effect on maximal binding (Bmax). This pharmacology appears to be specific for pre-synaptic H_3Rs and $A_{2A}Rs$, because we did not observe a similar decrease in $A_{2A}R$ affinity for CGS-21680 in membranes from the whole striatum, in which post-synaptic membranes constitute the major component (Figure 6D and Table 3).

4. Discussion

The H_3R has been proposed as a potential novel drug target for the treatment of drug use disorders, depression, schizophrenia, and Parkinson's disease. However, its wide brain expression and effects on other neurotransmitter systems may result in adverse effects when H_3R selective drugs are administered systemically. The $A_{2A}R$ has also been proposed as an option for the treatment of Parkinson's disease and possesses a strategic distribution in the striatum for targeting and modulating the cortico-dMSNs projections and the activity of iMSNs. The results presented herein may lead to an alternative to specifically target H_3Rs located in either iMSNs or cortical afferents synapsing onto dMSNs projections.

4.1 $A_{2A}R$-H_3R interaction

The primary finding of this study was the identification, for the first time, of $A_{2A}R$-H_3R heteromers, not only in recombinant cell systems but also in rat striatal nerve terminals.

The basis of the functional complementation assays requires a receptor to be nonfunctional and this was obtained by truncation of the C-terminus. Herein we showed that truncation of the H_3R from 445 to 411 or 421 residues was sufficient to prevent H_3R-mediated G protein activation of the H_3R-$G\alpha_{qi4}$ fusion protein, yet we were unable to functionally rescue its

signaling, indicating that the remaining C-tail may be too short to connect with an interacting GPCR. However, truncation to 427 amino acids allowed the H_3R to remain functional.

Exposure of HEK-293T cells transfected with H_3R_{427}-$G\alpha_{qi4}$ to the H_3R agonist RAMH resulted in Ca^{2+} mobilization (Figure 1E). As mentioned in the Results section, this response was not expected. In an optimal scenario, the receptor truncation would have prevented or diminished the receptor capability to activate G proteins and the H_3R_{427}-$G\alpha_{qi4}$ function was expected to be either complemented or increased by the co-expression and co-activation with the WT-H_3R. However, these conditions allowed for the detection of the loss of H_3R function with the solely presence of the $A_{2A}R$, suggesting a preference of the H_3R to form hetero-dimers over homo-dimers. It may be possible that truncating the H_3R at the amino acids 421–427 will result in a receptor short enough to abolish the homo/monomeric signaling, but long enough to functionally complement with a full length GPCR.

In order for a GPCR to activate G proteins, the integrity of helix 8 appears to be required. This structural requirement has been demonstrated for D_1Rs and opioid κ and μ receptors (van Rijn *et al.*, 2013). The H_3R third intracellular loop also appears to play a key role in the receptor-G protein coupling on the basis of the decreased signaling of the H_3R_{365} isoform, which lacks 80 residues in the third intracellular loop (Riddy *et al.*, 2016), and reduced signaling was induced by the A280V mutation in the same loop (Flores-Clemente *et al.*, 2013). Further consideration to the H_3R carboxyl tail should therefore be made when assessing the H_3R-G protein coupling.

An important issue when describing a novel heterodimer is to show changes in the signaling profiles of the receptors involved in the dimer. In this regard, we found enhanced signaling efficacy of the agonist CGS-21680 when the H_3R was co-transfected and co-activated in the HEK293T-$A_{2A}R$ cells. This effect can be explained by a H_3R-mediated facilitation of the $A_{2A}R$-G protein coupling, leading to an increase in the receptor efficacy to activate $G\alpha_s$ proteins and thus to produce cAMP. Given that in the absence of RAMH, CGS-21680 behaved the same in HEK293T-$A_{2A}R$ and HEK293T-$A_{2A}R$/H_3R cells, receptor expression does not appear to account for the observed effects.

Canonically H_3Rs couple to $G\alpha_{i/o}$ proteins, which inhibit adenylyl cyclase activity and accordingly activation of the receptor with RAMH lead to a decrease in cAMP formation. Similar to the observed in the Ca^{2+} mobilization assays, expression of the $A_{2A}R$ shifted the H_3R-mediated cAMP response from inhibition to an increase in the cAMP formation. In the Ca^{2+} mobilization assays we did not observe signaling of the H_3R through $G\alpha_{qs4}$ proteins bound to the truncated $A_{2A}R$, and we are thus not considering a H_3R change in signaling pathways as an explanation for this effect. Therefore, we hypothesized that in the $A_{2A}R$-H_3R heteromer the $A_{2A}R$ signaling prevails over that of the H_3R, hampered possibly by a steric impediment. This is in line with the loss of Ca^{2+} signaling when the H_3R-$G\alpha_{qi4}$ was co-expressed with the $A_{2A}R$.

An unexpected but interesting finding was the potential biased-signaling at the $A_{2A}R$-H_3R heteromer, as evidenced by the incapability of the endogenous ligand histamine to signal at

the $A_{2A}R$-H_3R heteromer compared to the exogenous agonist RAMH. This discrepancy suggests that RAMH induces conformational changes in the H_3R that allow the interaction to occur, whereas histamine-induced changes appear not sufficient for heteromerization, or at least for the heteromer to signal. Ligand bias could also be explained by agonist residence time, this is, the time that a particular drug remains in its binding pocket and that will directly determine the time that a given receptor maintains an active conformation. The active state induced by histamine may therefore have a shorter duration compared with that induced by RAMH, preventing the former from activating the chimeric G proteins bound to the $A_{2A}R_{302}$. Binding studies with striatal membranes and histamine show that the first hypothesis holds better because histamine induced an increase in the affinity of the $A_{2A}R$ for its agonist CGS-21680 (Supplementary Figure 4), opposite to the decrease in affinity change induced by RAMH in the same preparation. This result suggests that histamine and RAMH lock the H_3R in different conformational states that affect its interaction with the $A_{2A}R$.

4.2 Functional relevance of the $A_{2A}R$-H_3R heterodimer

Our results suggest a pre-synaptic location of the $A_{2A}R$-H_3R heterodimer in the striatum. A previous report indicates equal distribution of $A_{2A}Rs$ in total and synaptosomal membranes from rat striatum (Rebola *et al.*, 2005), with a preferential location on the post-synaptic density fraction over the pre-synaptic active zone fraction (49.2 ± 3.3 % and 26.9 ± 3.3 % of total immunoreactivity, respectively). H_3Rs are expressed pre- and post-synaptically (Ellenbroek and Ghiabi, 2014), but they seem to be highly enriched in the terminals of striato-pallidal neurons (iMSNs) yielding a value of 1,327 ± 79 fmol/mg protein (Morales-Figueroa e*t al.*, 2014). This distribution supports our proposal for the heterodimer location and suggests a role for the $A_{2A}R$-H_3R heteromer in the pre-synaptic modulation of glutamatergic and GABAergic transmission.

In the striatum, $A_{2A}Rs$ have a specific location in iMSNs (Schiffman *et al.*, 1991) and cortico-dMSNs terminals, but not in the cortico-iMSNs projections (Quiróz *et al.*, 2009) whereas the H_3R is ubiquitously expressed throughout the striatum (Nieto-Alamilla *et al.*, 2016). Both receptors can modulate the cortico-striatal glutamatergic and intra-striatal GABAergic transmission, but whereas the H_3R consistently inhibits neurotransmitter release in either location, the $A_{2A}R$ facilitates cortico-striatal glutamate release but inhibits GABA release from the iMSNs collaterals.

Our data depicts thus a scenario where the $A_{2A}R$ and the H_3R preserve their canonical signaling pathways ($G\alpha_s$ and $G\alpha_{i/o}$, respectively), and upon dimerization the H_3R facilitates the $A_{2A}R$ signaling. This receptor functionality is preserved in the cortico-dMSNs projections, with $A_{2A}R$ activation enhancing glutamate release (Popoli *et al.*, 1995) and H_3Rs exerting the opposite effect (Arias-Montaño *et al.*, 2001). Activation of the $A_{2A}R$-H_3R heterodimer in these terminals may further facilitate glutamate release, resulting in hyper-stimulation of the dMSNs population.

Contrary to the $A_{2A}R$ and H_3R antagonic modulation of glutamatergic transmission, both receptors inhibit GABA release from iMSNs collaterals. This may be due to the $A_{2A}R$ functional duality showed in this neuronal population, as demonstrated by its capability to activate $G\alpha_s$ and $G\alpha_q$ proteins (Gubitz *et al.*, 1995; Kirk and Richardson, 1996). Therefore,

we hypothesized that the activation of the $A_{2A}R$-H_3R heterodimer in this location will further inhibit GABA release from iMSN nerve terminals, facilitating the activation of the dMSNs. According to this hypothesis, the overall activation of the striatal $A_{2A}R$-H_3R heterodimer would increase dMSNs activity. It is therefore tempting to speculate that co-activation of the heterodimer may have relevance for the treatment of the autism and obsessive and compulsive disorder, in which alterations in cortico-striatal glutamatergic transmission and MSN excitability have been shown (Welch *et al.*, 2008; Naaijen *et al.*, 2017).

Furthermore, it has been reported that the $A_{2A}R$ antagonists KW-6002 and SCH-442416 can distinguish receptors located in the cortical afferents targeting dMSNs or iMSNs, respectively (Orrú *et al.*, 2011). Although there are no agonists capable to differentiate between $A_{2A}R$ populations, this information may be a valuable tool for targeting and modulating the $A_{2A}R$ and H_3R pharmacology in a location-specific manner, using bivalent ligands directed to the heterodimer.

5. Conclusion

This study presents for the first time evidence for an $A_{2A}R$-H_3R heterodimer based on functional complementation and co-immunoprecipitation assays in HEK-293 cells, where co-activation of the receptors leads to enhanced $A_{2A}R$ signaling and attenuation of H_3R functionality. In rat striatal tissue, the interaction occurs in synapses where H_3R activation modifies the binding affinity of the $A_{2A}R$.

Supplementary Material

Refer to Web version on PubMed Central for supplementary material.

Acknowledgements

We thank Juan Escamilla-Sánchez and Raúl González-Pantoja for excellent technical assistance. We also thank Sirenia González for help in obtaining the synaptosomal MET images. R. M.-G. held a Conacyt graduate scholarship (244993).

Funding

This work was supported by Cinvestav, Conacyt (grant 220448 to J.-A. A.-M.), PAPIIT-UNAM (grant IN216215 to J.-M. A.), the National Institute on Alcohol Abuse and Alcoholism (grant AA20539 to R. M. v R.) and the Ralph W. and Grace M. Showalter Research Trust (to R. M. v R.). The funding sources were not involved at all in the study design, collection, analysis and interpretation of data, writing of the manuscript or the decision to submit this report.

Abbreviations

$A_{2A}R$	Adenosine A_{2A} receptor
cAMP	Cyclic adenosine monophosphate
D_1R	Dopamine D_1 receptor
D_2R	Dopamine D_2 receptor

dMSNs	Direct pathway striatal medium-sized spiny neurons
GABA	γ-Aminobutyric acid
GPCRs	G-protein coupled receptors
H_2R	Histamine H_2 receptor
H_3R	Histamine H_3 receptor
H_4R	Histamine H_4 receptor
iMSNs	Indirect pathway striatal medium-sized spiny neurons
MSNs	Striatal medium-sized spiny neurons
RAMH	(R)-α-methylhistamine
WT	Wild type

6. References

1. Arias-Montaño JA, Floran B, Garcia M, Aceves J, Young JM, 2001 Histamine H_3 receptor-mediated inhibition of depolarization-induced, dopamine D_1 receptor-dependent release of [^{3}H]-gamma-aminobutyric acid from rat striatal slices. Br J Pharmacol 133:165–171 [PubMed: 11325806]
2. Berjukow S, Döring F, Froschmayr M, Grabner M, Glossmann H, Hering S, 1996 Endogenous calcium channels in human embryonic kidney (HEK293) cells. Br J Pharmacol 118:748–754 [PubMed: 8762103]
3. Bolam JP, Hanley JJ, Booth PA, Bevan MD, 2000 Synaptic organization of the basal ganglia. J Anat 196:527–542 [PubMed: 10923985]
4. Bolam PJ, Ellender TJ, 2016 Histamine and the striatum. Neuropharmacology 106:74–84 [PubMed: 26275849]
5. Cabello N, Gandía J, Bertarelli DCG, Watanabe M, Lluís C, Franco R, Ferré S, Luján R, Ciruela F, 2009 Metabotropic glutamate type 5, dopamine D_2 and adenosine A_{2a} receptors from higher-order oligomers in living cells. J Neurochem 109:1497–1507 [PubMed: 19344374]
6. Carriba P, Ortiz O, Patkar K, Justinova Z, Stroik J, Themann A, Muller C, Woods AS, Hope BT, Ciruela F, Casadó V, Canela EI, Lluis C, Goldberg SR, Moratalla R, Franco R, Ferré S, 2007 Striatal adenosine A_{2A} and cannabinoid CB_1 receptors form functional heteromeric complexes that mediate the motor effects of cannabinoids. Neuropsycopharmacology 32:2249–2259
7. Chiang T, Sansuk K, van Rijn RM, 2016 β-arrestin 2 dependence of δ opioid receptor agonists is correlated with alcohol intake. Br J Pharmacol 173:332–343 [PubMed: 26507558]
8. Ciruela F, Casadó V, Rodrigues RJ, Luján R, Burgueño J, Canals M, Borycz J, Rebola N, Goldberg SR, Mallol J, Cortés A, Canela EI, López-Giménez JF, Milligan G, Lluis C, Cunha RA, Ferré S, Franco R, 2006 Presynaptic control of striatal glutamatergic neurotransmission by adenosine A_1-A_{2A} receptor heteromers. J Neurosci 26:2080–2087 [PubMed: 16481441]
9. Cogé F, Guénin SP, Audinot V, Renouard-Try A, Beauverger P, Macia C, Ouvry C, Nagel N, Rique H, Boutin JA, Galizzi JP, 2001 Genomic organization and characterization of splice variants of the human histamine H_3 receptor. Biochem J 355:279–288 [PubMed: 11284713]
10. Conklin BR, Herzmark P, Ishida S, Voyno-Yasenetskaya TA, Sun Y, Farfel Z, Bourne HR, 1996 Carboxyl terminal mutations of Gq alpha and Gs alpha that alter the fidelity of receptor activation. Mol Pharmacol 50:885–890 [PubMed: 8863834]
11. Doreulee N, Yanovsky Y, Flagmeyer I, Stevens DR, Haas HL, Brown RE, 2001 Histamine H_3 receptors depress synaptic transmission in the corticostriatal pathway. Neuropharmacology 40:106–113 [PubMed: 11077076]

12. Ellenbroek BA, 2013 Histamine H_3 receptors, the complex interaction with dopamine and its implications for addiction. Br J Pharmacol 170:46–57 [PubMed: 23647606]
13. Ellenbroek BA, Ghiabi B, 2014 The other side of the histamine H_3 receptor. Trends Neurosci 37:191–199 [PubMed: 24636456]
14. Ferré S, Ciruela F, Canals M, Marcellino D, Burqueno J, Casadó V, Hillion J, Torvinen M, Fanelli F, Benedetti PD, Goldberg SR, Bouvier M, Fuxe K, Agnati LF, Lluis C, Franco R, Woods A, 2004 Adenosine A_{2A}-dopamine D_2 receptor-receptor heteromers. Targets for neuro-psychiatric disorders Parkinsonism. Relat Disord 10:265–271
15. Ferré S, Fredholm BB, Moreli M, Popoli P, Fuxe K, 1997 Adenosine-dopamine receptor-receptor interactions as an integrative mechanism in the basal ganglia. Trends Neurosci 20:482–487 [PubMed: 9347617]
16. Flores-Clemente C, Osorio-Espinoza A, Escamilla-Sánchez J, Leurs R, Arias JM, Arias-Montaño JA, 2013 A single-point mutation (Ala280Val) in the third intracellular loop alters the signaling properties of the human histamine H_3 receptor stably expressed in CHO-K1 cells. Br J Pharmacol 170:127–135 [PubMed: 23713487]
17. Gonzalez-Sepulveda M, Rosell S, Hoffman HM, del Mar. Castillo-Ruíz Ma., Mignon V, Moreno-Delgado D, Vignes M, Diaz J, Sabria J, Ortiz J, 2013 Cellular distribution of the histamine H_3 receptor in the basal ganglia: Functional modulation of dopamine and glutamate neurotransmission. Basal Ganglia 3:109–121
18. Gubitz AK, Widdowson L, Kurokawa M, Kirkpatrick KA, Richardson PJ, 1996 Dual signaling by the adenosine A_{2a} receptor involves activation of both N- and P-type calcium channels by different G proteins and protein kinases in the same striatal nerve terminals. J Neurochem 67:374–381 [PubMed: 8667016]
19. Han Y, Moreira IS, Urizar E, Weinstein H, Javitch JA, 2009 Allosteric communication between protomers of dopamine class A GPCR dimers modulates activation. Nat Chem Biol 5:688–695 [PubMed: 19648932]
20. Hillion J, Canals M, Torvinen M, Casado V, Scott R, Terasmaa A, Hansson A, Watson S, Olah ME, Canela EI, Zoli M, Agnati LF, Ibanez CF, Lluis C, Franco R, Ferre S, Fuxe K, 2002 Coaggregation, cointernalization, and codesensitization of adenosine A_{2A} receptors and dopamine D_2 receptors. J Biol Chem 277:18091–18097 [PubMed: 11872740]
21. Kemp JM, Powell TP, 1971 The structure of caudate nucleus of the cat: light and electron microscopy. Philos Trans R Sot Lond B Biol Sci 262:383–401.
22. Kirk IP and Richardson PJ, 1994 Adenosine A_{2a} receptor-mediated modulation of striatal [^{3}H]GABA and [^{3}H]acetylcholine release. J Neurochem 62:960–966 [PubMed: 8113816]
23. Kirk IP, Richardson PJ, 1995 Inhibition of striatal GABA release by the adenosine A_{2A} receptor is not mediated by increase in cyclic AMP. J Neurochem 64:2801–2808 [PubMed: 7760061]
24. Márquez-Gómez R, Gutierrez-Rodelo C, Robins MT, Escamilla-Sánchez J, Olivares-Reyes J-A, van Rijn R, Arias-Montaño J-A, 2016 On the existence of a histamine H_3–adenosine A_{2A} receptor heteromer. Inflamm Res 65 (Suppl. 1), S29
25. Marquez-Gomez R, Gutierrez-Rodelo C, Robins MT, Arias J-M, Olivares-Reyes J-A, van Rijn RM, Arias-Montaño J-A, 2017 Functional histamine H3 and adenosine A2A receptor heteromers in recombinant cells and rat striatum. bioRxiv 171736; doi: 10.1101/171736
26. Morales-Figueroa GE, Márquez-Gómez R, González-Pantoja R, Escamilla-Sanchez J, Arias-Montaño JA, 2015 Histamine H_3 receptor activation counteracts adenosine A_{2A} receptor-mediated enhancement of depolarization-evoked [^{3}H]-GABA release from rat globus pallidus synaptosomes. ACS Chem Neurosci 20:637–645
27. Moreno E, Moreno-Delgado D, Navarro G, Hoffmann HM, Fuentes S, Rosell-Vilar S, Gasperini P, Rodriguez-Ruiz M, Medrano M, Mallol J, Cortés A, Casadó V, Lluis C, Ferré S, Ortiz J, Canela E, McCormick PJ, 2014 Cocaine disrupts histamine H_3 receptor modulation of dopamine D_1 receptor signaling: σ_1-D_1-H_3 receptor complexes as key targets for reducing cocaine's effects. J Neurosci 34:3545–3558 [PubMed: 24599455]
28. Naaijen J, Zwier MP, Amiri H, Williams SCR, Durston S, Oranje B, Brandeis D, Boecker-Schlier R, Ruf M, Wolf I, Banaschewski T, Glennon JC, Franke B, Buitelaar JK, Lythgoe DJ, 2017

Fronto-striatal glutamate in autism spectrum disorders and obsessive compulsive disorder. Neuropsychopharmacology 42:2456–2465 [PubMed: 27869141]

29. Nieto-Alamilla G, Márquez-Gómez R, García-Gálvez A-M, Morales-Figueroa G-E, Arias-Montaño J-A, 2016 The histamine H_3 receptor: structure, pharmacology and function. Mol Pharmacol 90:649–673 [PubMed: 27563055]
30. Panula P, Nuutinen S, 2013 The histaminergic network in the brain: basic organization and role in disease. Nat Rev Neurosci 14:472–487 [PubMed: 23783198]
31. Panula P, Chazot PL, Cowart M, Gutzmer R, Leurs R, Liu WLS, Stark H, Thurmond RL, Haas HL, Ohlstein EH, 2015 International union of basic and clinical pharmacology. XCVIII. Histamine receptors. Pharmacol Rev 67:601–655 [PubMed: 26084539]
32. Passani MB, Blandina P, 2011 Histamine receptors in the CNS as target for therapeutic intervention. Trends Pharmacol Sci 32:242–249 [PubMed: 21324537]
33. Pillot C, Heron A, Cochois V, Tardivel-Lacombe J, Ligneau X, Schwartz J-C, Arrang J-M, 2002 A detailed mapping of the histamine H_3 receptor and its gene transcripts in rat brain. Neuroscience 114:173–193 [PubMed: 12207964]
34. Popoli P, Betto P, Reggio R, Ricciarello G, 1995 Adenosine A_{2A} receptor stimulation enhances striatal extracellular glutamate levels in rats. Eur J Pharmacol 287:215–217 [PubMed: 8749040]
35. Prast H, Tran MH, Fischer H, Kraus M, Lamberti C, Grass K, Philippu A, 1999 Histaminergic neurons modulate acetylcholine release in the ventral striatum: role of H_3 histamine receptors. Naunyn Schmiedebergs Arch Pharmacol 360:558–564 [PubMed: 10598795]
36. Quiroz C, Luján R, Chigashima M, Simoes AP, Lerner TN, Borycz J, Kachroo A, Canas PM, Orru M, Schwarzschild MA, Rosin DL, Kreitzer AC, Cunha RA, Watanabe M, Ferré S, 2009 Key modulatory role of presynaptic adenosine A_{2A} receptors in cortical neurotransmission to the striatal direct pathway. Scientific World Journal 18:1321–1344
37. Riddy DM, Cook AE, Diepenhorst NA, Bosnyak S, Brady R, Mannoury la Cour C, Mocaer E, Summers RJ, Charman WN, Sexton PM, Christopoulos A, Langmead CJ, 2016 Isoform-specific biased agonism of histamine H_3 receptor agonists. Mol Pharmacol 91:87–99 [PubMed: 27864425]
38. Rivera-Ramírez N, Montejo-López W, López-Méndez MC, Guerrero-Hernández A, Molina-Hernández A, García-Hernández U, Arias-Montaño JA, 2016 Histamine H3 receptor activation stimulates calcium mobilization in a subpopulation of rat striatal neurons in primary culture, but not in synaptosomes. Neurochem Int 101:38–47 [PubMed: 27744004]
39. Rodríguez-Ruiz M, Moreno E, Moreno-Delgado D, Navarro G, Mallol J, Cortés A, Lluís C, Canela EI, Casadó V, McCormick PJ, Franco R, 2017 Heteroreceptor complexes formed by dopamine D_1, histamine H_3, and N-Methyl-D-Aspartate glutamate receptors as targets to prevent neuronal death in Alzheimer's disease. Mol Neurobiol 54:4537–4550 [PubMed: 27370794]
40. Schiffmann SN, Jacobs O, Vanderhaeghen JJ, 1991 Striatal restricted adenosine A_2 receptor (RDC8) is expressed by enkephalin but not by substance P neurons: an in situ hybridization histochemistry study. J Neurochem 57:1062–1067 [PubMed: 1713612]
41. Schliker E, Fink K, Detzner M, Gothert M, 1993 Histamine inhibits dopamine release in the mouse striatum via presynaptic H_3 receptors. J Neural Transm Gen Sect 93:1–10 [PubMed: 8396945]
42. Schwarzschild MA, Agnati L, Fuxe K, Chen JF, Morelli M, 2006 Targeting adenosine A_{2A} receptor in Parkinson's disease. Trends Neurosci 29:647–654 [PubMed: 17030429]
43. Tapper JM, Kóos T, Wilson CJ, 2004 GABAergic microcircuits in the neostriatum. Trends Neurosci 27:662–669. [PubMed: 15474166]
44. Thomas P, Smart TG, 2005 HEK293 cells line: A vehicle for the expression of recombinant proteins. J Pharmacol and Toxicol Methods 51:187–200 [PubMed: 15862464]
45. van Rijn RM, Harvey JH, Brissett DI, DeFriel JN, Whistler JL, 2013 Novel screening assay for the selective detection of G-protein-coupled receptor heteromer signaling. J Pharmacol Exp Ther 344:179–188 [PubMed: 23097213]
46. Welch JM, Lu J, Rodriguez RM, Trotta NC, Peca J, Ding J-D, Feliciano C, Chen M, Adams JP, Luo J, Dudek SM, Weinberg RJ, Calakos N, Wetsel WC, Feng G, 2008 Cortico-striatal synaptic defects and OCD-like behaviors in SPAP3 mutant mice. Nature 448:894–900

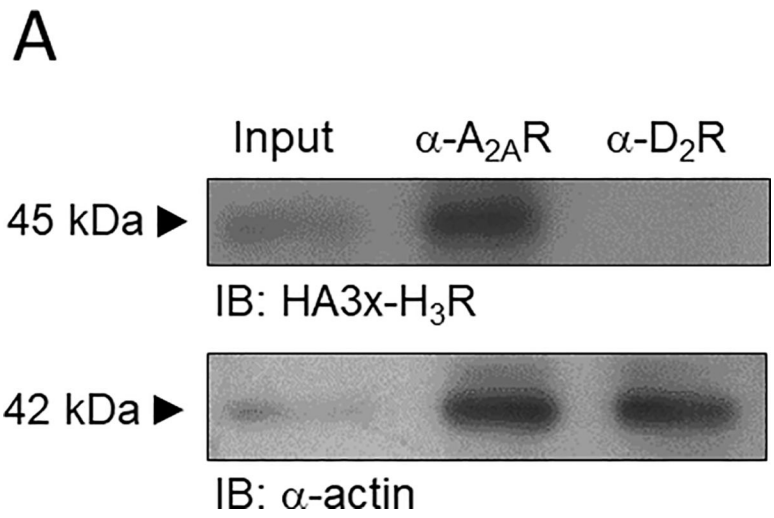

Figure 1.

Adenosine A_{2A} and histamine H_3 receptors co-immunoprecipitate in transfected HEK-293 cells. A. Co-immunoprecipitation of the hemagglutinin-tagged H_3R (3xHA-H_3R) with the $A_{2A}R$ in protein extracts from HEK-293 cells. The ~45 kDa band corresponds to the 3xHA-H_3R, and was not observed with the negative control. Input represents 30% of the total protein. An antibody against the D_2 receptor (α-D_2R) was used as a negative control. The blot is representative of 3 independent experiments. The whole blot is shown in Supplementary Figure 5.

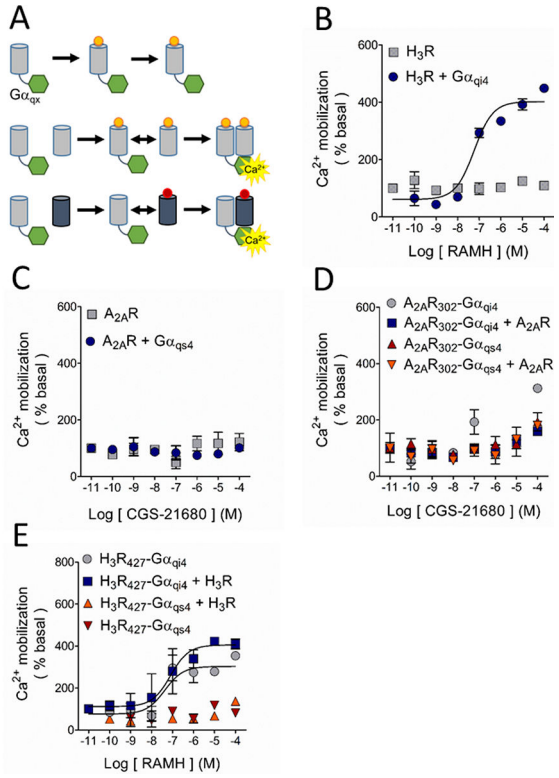

Figure 2.

Study of the possible $A_{2A}R$-H_3R dimerization by functional complementation assay. A. Basis of the assay. The G protein-coupled receptor (GPCR; grey cylinders) is truncated at its carboxyl terminus to generate a nonfunctional GPCR, which is then fused to the chimeric G protein (green hexagons). The chimeric G protein is formed by a $G\alpha_q$ protein in which 9 or 10 residues of the C-terminus were substituted by the corresponding sequence of a $G\alpha_{s4}$ or $G\alpha_{i4}$ protein (represented by X). Under these conditions, Ca^{2+} mobilization can only be elicited when the complex GPCR-$G\alpha_{qx}$ is in close proximity to a wild type (WT) GPCR, either the same (homodimerization) or a different receptor (heterodimerization). B. Activation of the H_3R with its agonist RAMH resulted in Ca^{2+} mobilization only when it was co-expressed with the chimeric $G\alpha_{qi4}$ but not when transfected alone. C. When activated with its agonist CGS-21680, the $A_{2A}R$ was uncapable to induce Ca^{2+} mobilization either alone or when co-transfected with the chimeric $G\alpha_{qs4}$ protein. D. Functional complementation by homodimerization of the truncated $A_{2A}R_{302}$, either bound to $G\alpha_{qs4}$ ($A_{2A}R_{302}$-$G\alpha_{qs4}$) or $G\alpha_{qi4}$ ($A_{2A}R_{302}$-$G\alpha_{qi4}$), with the native $A_{2A}R$ was not observed. E. Activation of the truncated H_3R_{427} bound to $G\alpha_{qi4}$ (H_3R_{427}-$G\alpha_{qi4}$) induced Ca^{2+} mobilization on its own and homodimerization with the WT-H_3R did not modify the response. No signal was observed with activation of the H_3R_{427}-$G\alpha_{qs4}$ construct when it was co-expressed with the WT-H_3R. In all graphs data are means ± SEM from 3 replicates from a representative experiment. Where SEM bars are not visible, they are smaller than the symbol size. The quantitative analysis is shown in Tables 1 and Supplementary Table 2.

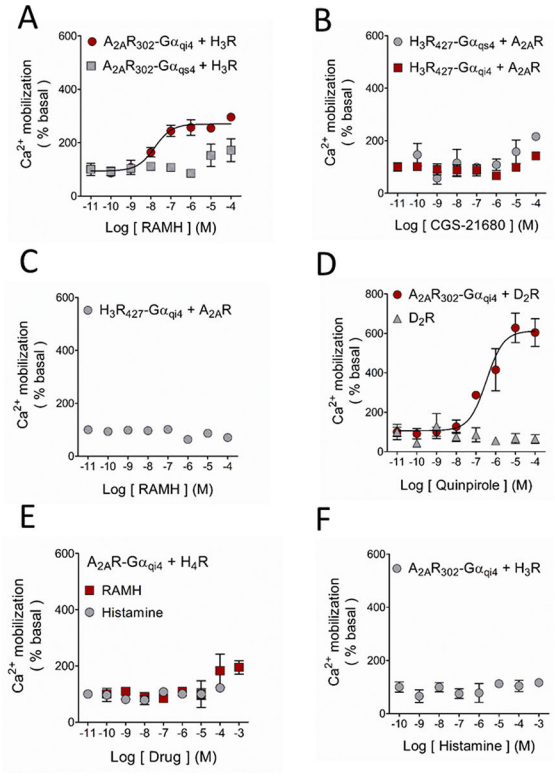

Figure 3.

Ligand modulation of the $A_{2A}R$-H_3R interaction in HEK-293 cells. Activation of the WT-H_3R with its agonist RAMH led to functional complementation when co-expressed with the $A_{2A}R_{302}$-Gαqi4 but not with $A_{2A}R_{302}$-Gαqs4. B. Ca^{2+} mobilization was not observed when the WT-$A_{2A}R$ was co-transfected with the truncated H_3R_{427}-Gαqs4 or H_3R_{427}-Gαqi4, in accord with the incapability of the receptor to activate the chimeric proteins. C. As shown in Figure 1D, activation of the H_3R_{427}-Gαqi4 resulted in Ca^{2+} mobilization, and this response was prevented when it was co-expressed with the WT-$A_{2A}R$, suggesting a preference of the H_3R_{427}-Gαqi4 to form heterodimers. D. The well-studied $A_{2A}R$-D_2R heterodimer was used as a positive control for these experiments. Activation of the D_2R with increasing concentrations of the agonist quinpirole caused marked Ca^{2+} mobilization only when co-expressed with the chimeric $A_{2A}R_{302}$-Gαqi4. E. The histamine H_4 receptor (H_4R) as a negative control. No functional complementation was observed when the receptor was co-expressed with the $A_{2A}R_{302}$-Gαqi4, showing the specificity of the $A_{2A}R$-H_3R interaction. F. Functional complementation between the $A_{2A}R_{302}$-Gαqi4 and the WT-H_3R was not observed when the latter receptor was activated with the endogenous agonist histamine. For all graphs data are means ± SEM from 3 replicates from representative experiments. Where SEM bars are not visible, they are smaller than the symbol size. The quantitative analysis is shown in Table 1 and Supplementary Table 2.

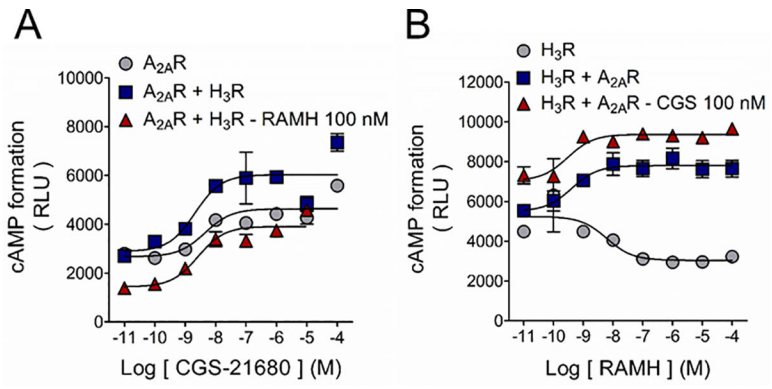

Figure 4.

H_3R activation enhances $A_{2A}R$-mediated cAMP signaling in HEK-293 cells. A. Activation of the $G\alpha_s$-coupled $A_{2A}R$ with its agonist CGS-21680 induced cAMP formation and H_3R co-activation enhanced $A_{2A}R$ efficacy. Co-expression of the H_3R did not modified the $A_{2A}R$ functional response. Values for pEC_{50} and maximal effect (Emax) are given in Table 2. B. H_3R activation with RAMH decreased forskolin-induced cAMP formation in accord with the inhibitory nature of the $G\alpha_{i/o}$-coupled receptor. $A_{2A}R$ expression and receptors co-activation lead to a change in the H_3R signaling. Data are means ± SEM from 5 replicates from a representative experiments. Where SEM bars are not visible, they are smaller than the symbol size. Values for pIC_{50} and maximal effect (Imax) are given in Table 2.

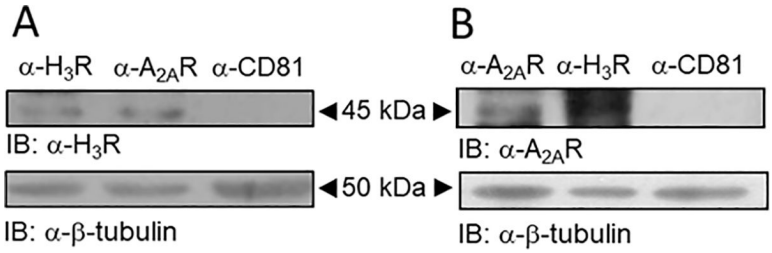

Figure 5.

Co-immunoprecipitation of the A_{2A} and H_3 receptors in striatal synaptosomes. A. The H_3R co-immunoprecipitated with the $A_{2A}R$ in a protein extract of Percoll-purified striatal synaptosomes. The band of ~45 kDa corresponds to the expected migration of the H_3R. No band was observed in the negative control (α-CD81). B. Co-immunoprecipitation of the $A_{2A}R$ with the H_3R in a protein extract of striatal synaptosomes. The band of ~45 kDa corresponds to the expected migration of the $A_{2A}R$. The figure depicts representative blots, repeated a further 4 times with similar results. Full blots are shown in Supplementary Figure 6.

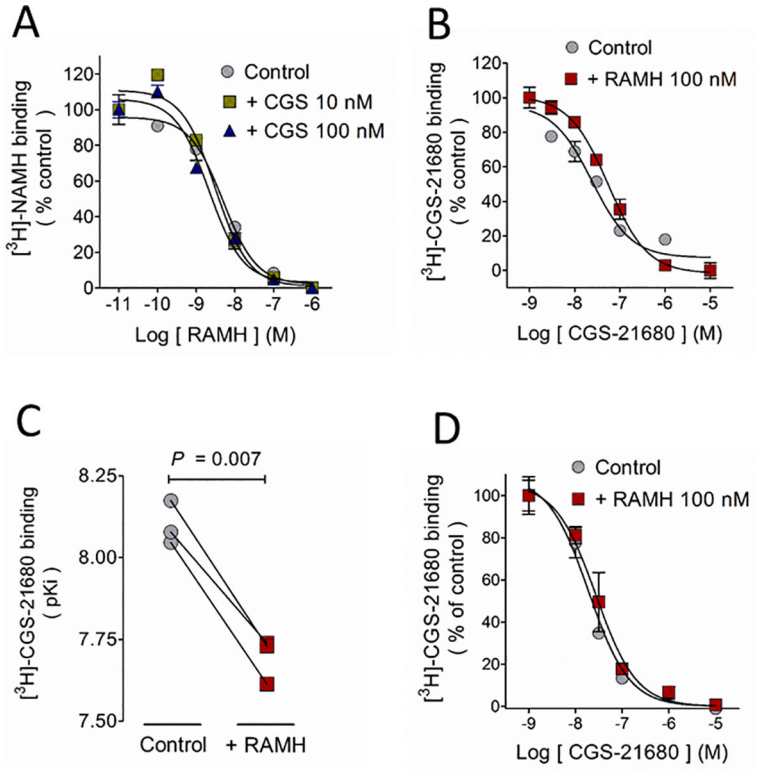

Figure 6.

H_3R activation decreases $A_{2A}R$ affinity for the agonist CGS-21680 in synaptosomal membranes but not in membranes from the whole striatum A. CGS-21680 (10 and 100 nM) did not modify the H_3R affinity for its ligand RAMH in membranes isolated from striatal synaptosomes. B. In the same preparation, the H_3R agonist RAMH (100 nM) decreased the $A_{2A}R$ affinity for [^{3}H]-CGS-21680. Values are means ± SEM from 3 replicates from a representative experiment. C. Analysis of 3 independent experiments. The statistical analysis was performed with paired Student's *t* test. D. H_3R activation with RAMH (100 nM) failed to decreased the $A_{2A}R$ affinity for [^{3}H]-CGS-21680 in membranes from the whole striatum. Values are means ± SEM from 3 replicates from a representative experiment. Where SEM bars are not visible, they are smaller than the symbol size.

Table 1.

Pharmacological characteristics of the $A_{2A}R$-H_3R functional complementation assays in transfected HEK-293 cells

Transfection	Agonist	Emax (%)	pEC_{50}
$H_3R + G\alpha_{qi4}$	RAMH	419 ± 25	7.73 ± 0.31
	Histamine	504 ± 22[b]	6.19 ± 0.17[b]
H_3R_{427}-$G\alpha_{qi4}$	RAMH	753 ± 41	7.14 ± 0.21
H_3R_{427}-$G\alpha_{qi4}$ + H_3R	RAMH	523 ± 41b	7.38 ± 0.34
$A_{2A}R_{302}$-$G\alpha_{qi4}$ + H_3R	RAMH	449 ± 25	7.31 ± 0.23
	RAMH + CGS	429 ± 14[ns]	7.63 ± 0.15
$H_4R + G\alpha_{qi4}$	Histamine	725 ± 51	6.35 ± 0.25
	RAMH	551 ± 27[a]	6.15 ± 0.16
$H_2R + G\alpha_{qs4}$	Dimaprit	860 ± 37	6.15 ± 0.12
$A_{2A}R_{302}$-$G\alpha_{qi4}$ + D_2R	Quinpirole	612 ± 34	6.47 ± 0.22

Data are means ± SEM from 3 experiments. Statistical comparisons were performed between two agonists for the same transfection, or between the transfection with the chimeric receptor and the transfection of the chimeric receptor plus the wild type receptor. ns, no significant difference

[a] $P < 0.05$

[b] $P < 0.01$, Student's *t* test.

Both RAMH and CGS-21680 were assayed at 100 nM. RAMH, R-α-methylhistamine; CGS, CGS-21680.

Table 2.

Pharmacological characteristics of the cAMP formation assay in transfected HEK-293 cells.

Transfection	Agonist	pEC_{50}	Emax (%)	pIC_{50}	Imax (%)
$A_{2A}R$	CGS	8.0 ± 0.4	152 ± 7	-	-
$A_{2A}R + H_3R$	CGS	8.7 ± 0.5	153 ± 7	-	-
$A_{2A}R + H_3R$	+RAMH	8.0 ± 0.2	248 ± 9[b]	-	-
H_3R	RAMH	-	-	8.1 ± 0.3	−26 ± 2
$H_3R \pm A_{2A}R$	RAMH	10.6 ± 1	114 ± 3	-	-
$H_3R \pm A_{2A}R$	+CGS	9.9 ± 0.6	120 ± 2	-	-

Data are means ± SEM from 3 experiments. Statistical comparisons were performed between two agonists for the same transfection, or between the transfection with the chimeric receptor and the transfection of the chimeric receptor plus the wild type receptor. ns, no significant difference

[a] $P < 0.05$

[b] $P < 0.01$, Student's *t* test.

Both RAMH and CGS-21680 were assayed at 100 nM. RAMH, R-α-methylhistamine; CGS, CGS-21680.

Table 3.

Analysis of binding assays in rat striatal membranes

	pKi	Bmax (%)
[^{3}H]-NAMH		
Synaptosomes		
RAMH	9.09 ± 0.22	100.0 ± 0.3
RAMH + CGS 10 nM	8.99 ± 0.02^{ns}	110.0 ± 4.0^{ns}
RAMH + CGS 100 nM	9.08 ± 0.06^{ns}	103.0 ± 4.1^{ns}
[^{3}H]CGS-21680		
Whole striatum		
CGS	8.06 ± 0.15	100.0 ± 14
CGS + RAMH	8.11 ± 0.04^{ns}	88.0 ± 6.0^{ns}
Synaptosomes		
CGS	8.10 ± 0.04	100.0 ± 9.0
CGS + RAMH	7.70 ± 0.04^{a}	88.1 ± 10.0^{ns}

Data are means ± SEM from 3–5 experiments. For [^{3}H]-NAMH binding assays the statistical analysis was performed with one-way Anova and Dunnett´s *post hoc* test. For [^{3}H]-CGS-21680 binding, values in the presence of RAMH were compared with the corresponding control with Student's *t* test.

$^{a}P < 0.001$, ns, not significant. CGS, CGS-21680. RAMH (R-α-methylhistamine) was tested at 100 nM in all the experiments.